Orange Organic Long-persistent Luminescence from an Electron Donor/Acceptor Binary System

Zesen Lin[1,2,3], Ryota Kabe*[1,2,3], and Chihaya Adachi*[1,2,4]

[1] *Center for Organic Photonics and Electronics Research (OPERA), Kyushu University*
744 Motooka, Nishi-ku, Fukuoka, 819-0395, Japan.

[2] *JST, ERATO Adachi Molecular Exciton Engineering Project, Kyushu University*
744 Motooka, Nishi-ku, Fukuoka 819-0395, Japan.

[3] *Okinawa Institute of Science and Technology Graduate University*
1919-1 Tancha, Onna-son, Kunigami-gun, Okinawa 904-0495, Japan.

[4] *International Institute for Carbon Neutral Energy Research (WPI-I2CNER), Kyushu University*
744 Motooka, Nishi-ku, Fukuoka, 819-0395, Japan.

E-mail: ryota.kabe@oist.jp; adachi@opera.kyushu-u.ac.jp

1   Organic long-persistent luminescence (LPL) materials
2 can overcome the disadvantages of inorganic LPL materials
3 in terms of element sustainability, processability, and color
4 tunability. However, all published electron donor/acceptor
5 binary organic LPL systems show green emission. Here, we
6 report an organic LPL system consisting of *N,N,N',N'*-
7 tetrakis(*p*-diisobutylaminophenyl)-*p*-phenylenediamine
8 (TBAPD) as a donor dopant and *2,8*-
9 bis(diphenylphosphoryl)dibenzo[b,d]thiophene (PPT) as an
10 acceptor host. The TBAPD/PPT film exhibits orange
11 photoluminescence (CIE_x, CIE_y = 0.49, 0.49) and LPL (CIE_x,
12 CIE_y = 0.51, 0.48).

14 Keywords: Organic long-persistent luminescence,
15 Exciplex, Charge separation

16   Long-persistent luminescence (LPL) materials, also
17 known as glow-in-the-dark or afterglow materials, are
18 widely used in emergency signs, watch indicators, safety
19 way guidance, and afterglow toys.[1-4] Glow-in-the-dark
20 materials have a long history of usage, and LPL materials
21 have been commonly used since Matsuzawa et al. developed
22 a strontium aluminate-based LPL material in the 1990s.[5]
23 Many commercial high-performance LPL materials are
24 made from metal oxides doped with rare earth elements
25 such as europium and dysprosium.[1] These inorganic LPL
26 materials need high fabrication temperatures of over
27 1000 °C and to be ground into powders and blended with
28 polymers for the majority of their applications.[1,6,7]
29   In 2017, we reported the first genuine organic LPL
30 (OLPL) system consisting of an electron donor *N,N,N',N'*-
31 tetramethylbenzidine (TMB) and an electron acceptor *2,8*-
32 bis(diphenylphosphoryl)dibenzo[b,d]thiophene (PPT).[8] This
33 TMB/PPT blend film exhibits LPL for over one hour at
34 room temperature when the concentration of the donor is
35 low (1 mol%). The LPL emission originates from the
36 excited state complex (exciplex) generated by the slow
37 recombination of long-lived intermediate charge-separated
38 (CS) states (Figure 1a). Initially, charge transfer (CT)
39 excited states ($D^{\delta+} + A^{\delta-}$) are formed between the donor (D)
40 and acceptor (A) during photo-excitation. Although most of
41 the CT excited states exhibit photoluminescence after turn-
42 off of the photoexcitation, some electrons on acceptors
43 diffuse to surrounding acceptor molecules and form stable

44 charge-separated (CS) states ($D^{\cdot+} + A^{\cdot-}$). Gradual
45 recombination of the electrons on the acceptor and holes on
46 the donor continuously generates CT excited states, so the
47 photoluminescence continues for a very long time. The
48 TMB/PPT film exhibits green LPL emission because the
49 exciplex emission corresponds to a transition from the
50 lowest unoccupied molecular orbital (LUMO) level of the
51 acceptor to the highest occupied molecular orbital (HOMO)
52 level of the donor. Although the donor-acceptor distance
53 and molecular conformations affect the exciplex emission,
54 the HOMO-LUMO gap play a decisive role in the exciplex
55 emission in the amorphous solid-state. A linear correlation
56 between the exciplex emission peak and the energy gap
57 between the oxidation potential of donors and the reduction
58 potential of acceptors ($E_{A,LUMO} - E_{D,HOMO}$) is reported[9-12] and
59 the HOMO and LUMO levels can be calculated from the
60 oxidation and reduction potentials.[13,14] The LPL emission
61 decay profile follows power-law decay, and the emission
62 intensity at time *t* is given by $I(t) \sim t^{-m}$, with m $\approx$ −1.[15-19]
63 This power-law emission decay differs from general room-
64 temperature phosphorescence which exhibits exponential
65 emission decay.[20-28]
66   We also reported several electron donor/acceptor
67 binary OLPL systems such as *m*-MTDATA/PPT[29] and
68 polymer-based TMB/PBPO.[7] However, these binary OLPL
69 systems exhibit green emission. Other emission-color
70 systems have not been reported. Later, we also achieved
71 wide-range emission-color tuning from greenish-blue to red
72 and even warm white by energy transfer from the TMB/PPT
73 exciplex to additional emitter dopants.[30] The color-tuning of
74 the binary OLPL system is important because the photo-
75 absorption process is controlled by the donor or acceptor
76 molecules. A large overlap between the exciplex emission
77 and the extra dopant absorption is required for efficient
78 energy transfer.
79   Here, we report orange LPL emission from a
80 donor/acceptor binary system. To obtain a longer emission
81 wavelength from the exciplex, we adjusted the HOMO level
82 of the donor from that of TMB. Specifically, *N,N,N',N'*-
83 tetra(*4*-tolyl)-*1,4*-phenylenediamine (TTPD) and *N,N,N',N'*-
84 tetrakis[(4-(diisobutylamino)phenyl]-*1,4*-phenylenediamine
85 (TBAPD) (Figure 1b) are used as donors in this study.
86   TTPD was synthesized by Buchwald-Hartwig coupling
87 and PPT was synthesized according to the literature.[31]

88 TBAPD was obtained from TCI chemicals (Tokyo, Japan).
89 All samples were purified by train sublimation. The 0.4
90 mm-thick TTPD/PPT and TBAPD/PPT films for the optical

91 measurements were prepared by the melt-casting method as
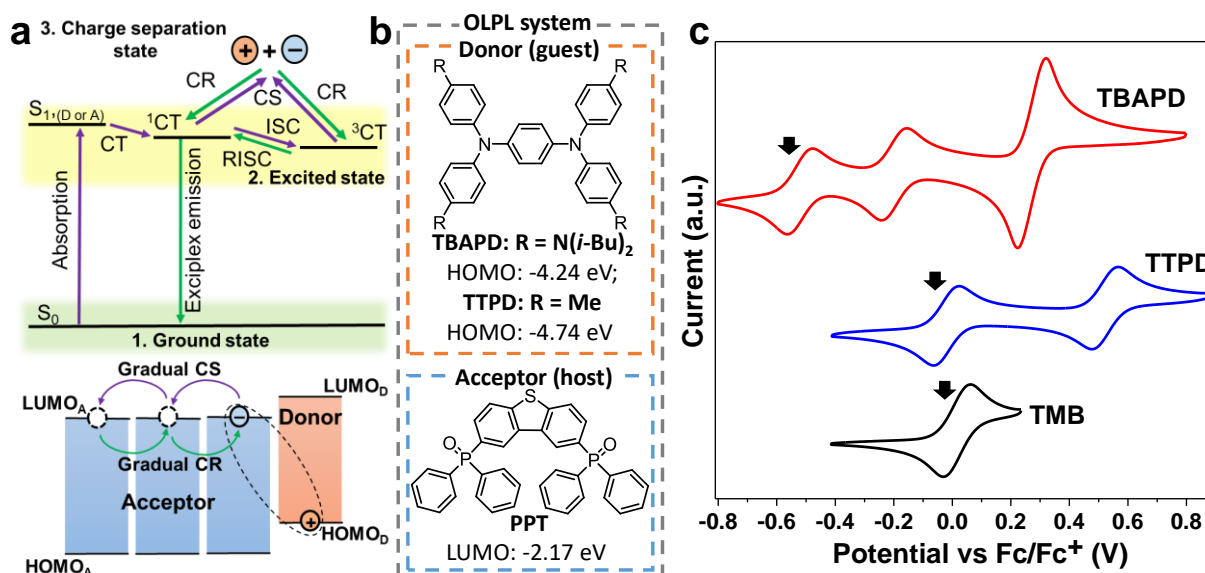92 reported previously.[30] Thin films for the UV-vis absorption

93
94 **Figure 1. a**. Emission mechanism of an OLPL. The dashed cycle represents the charge transfer (CT) exciton of the exciplex.
95 Abbreviations of electron donor (D), acceptor (A), lowest singlet excited state of donor or acceptor ($S_{1, (D\ or\ A)}$), CT singlet (^{1}CT)
96 and triplet excited state (^{3}CT), intersystem crossing (ISC), reverse intersystem crossing (RISC), charge separation (CS), and charge
97 recombination (CR) are used. **b**. Chemical structures of the electron donors (TTPD and TBAPD) and electron acceptor (PPT) and
98 their corresponding HOMO or LUMO levels. **c**. CV curves of TMB, TTPD, and TBAPD.

99 measurements were fabricated by sandwiching the heat-
100 melted materials between two quartz substrates. The
101 concentration of the donor was 1 mol% for all films,
102 according to the previous publication[8].
103   To achieve a longer emission wavelength, a shallower
104 HOMO level of the donor is required. Therefore, we
105 introduced electron-donating diisobutylamino substitutions
106 into the *N,N,N',N'*-tetraphenyl-*1,4*-phenylenediamine core,
107 and tetramethyl substitutions are used as the reference. The
108 HOMO levels were calculated to be -4.78 eV (TMB), -4.74
109 eV (TTPD), and -4.24 eV (TBAPD) from the first oxidation
110 potential of cyclic voltammograms. Although the TBAPD
111 and TTPD exhibit multi redox potentials, only the first
112 redox potential is important to discuss the LPL emission
113 since the system generates the radical cation of donors and
114 the radical anion of acceptors after the photoexcitation. The
115 LUMO level of PPT is -2.17 eV,[30] and the $E_{A,LUMO} -$
116 $E_{D,HOMO}$ of the donor/acceptor systems were calculated to be
117 2.61 eV (TMB/PPT), 2.57 eV (TTPD/PPT), and 2.07 eV
118 (TBAPD/PPT). The energy gap of 2.07 eV corresponds to
119 emission at 599 nm, so TBAPD/PPT should exhibit yellow
120 to orange emission.
121   UV-vis absorption and photoluminescence spectra of
122 TTPD and TBAPD (toluene solutions), and PPT,
123 TTPD/PPT, and TBAPD/PPT films are shown in Figure 2.
124 LPL spectra of these two blend films are also shown. The
125 absorption of the two blend films is the sum of the
126 absorption of PPT and the corresponding donor and could

127 not observe clear CT absorption at the present condition.
128 Thus, the charge-transfer interaction at the ground state is
129 almost negligible. In contrast, the TTPD/PPT and
130 TBAPD/PPT films exhibit broad emission peak maxima at
131 506 nm and 579 nm, respectively. These peak maxima are
132 significantly redshifted compared with the fluorescence and
133 phosphorescence of PPT and the corresponding donor.
134 These emission peaks clearly indicate that the emission of
135 the two blend films originates from the exciplex. The LPL
136 spectra are slightly redshifted and broader than the
137 corresponding steady-state photoluminescence spectra. This
138 may be because of the reorganization of the emitters at the
139 excited states.
140   The photoluminescence peak maxima of the
141 TTPD/PPT and TBAPD/PPT systems are at 506 nm and 579
142 nm, corresponding to energy gaps of 2.45 eV and 2.14 eV,
143 respectively. These values show good agreement with the
144 $E_{A,LUMO} - E_{D,HOMO}$ determined from the CV curves. As
145 expected, the TTPD/PPT system exhibits green
146 photoluminescence ($CIE_{x,y}$: 0.26, 0.46) and LPL ($CIE_{x,y}$:
147 0.31, 0.50), and the TBAPD/PPT system exhibits orange
148 photoluminescence ($CIE_{x,y}$: 0.49, 0.49) and LPL ($CIE_{x,y}$:
149 0.51, 0.48), as shown in Figure S1.
150   The LPL emission decay profiles of 1 mol% TMB/PPT,
151 TTPD/PPT, and TBAPD/PPT blend films under the same
152 excitation conditions are shown in Figure 3. After stopping
153 the photo-excitation, all films exhibit LPL emission with a
154 power-law decay profile at room temperature. The 1 mol%

3

TBAPD/PPT film exhibits orange LPL emission, which can be recorded for several minutes using a charge-coupled-device camera. Owing to the very thick film of 0.4 nm, several cracks formed during the rapid cooling process.

Because the photoluminescence quantum yields (Φ_{PL}) measured under nitrogen atmosphere were 16% (TBAPD/PPT), 24% (TMB/PPT) and 41% (TTPD/PPT), the study-state PL intensities under photoexcitation shows the same order. In contrast, the LPL duration of TMB/PPT and
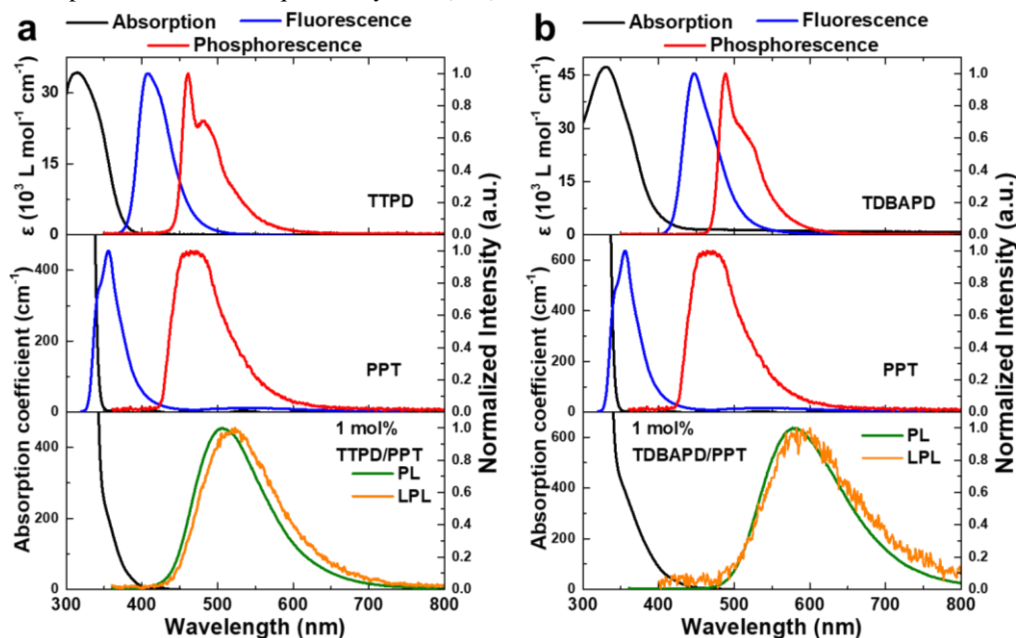
Figure 2. a, b. UV–vis absorption and photoluminescence spectra of TTPD and TBAPD in toluene (top), PPT film (middle), and 1 mol% TTPD/PPT and TBAPD/PPT films (bottom). The phosphorescence spectra were obtained at 77 K. The photoluminescence (PL) and LPL spectra of 1 mol% TTPD/PPT and TBAPD/PPT films were obtained at 300 K.
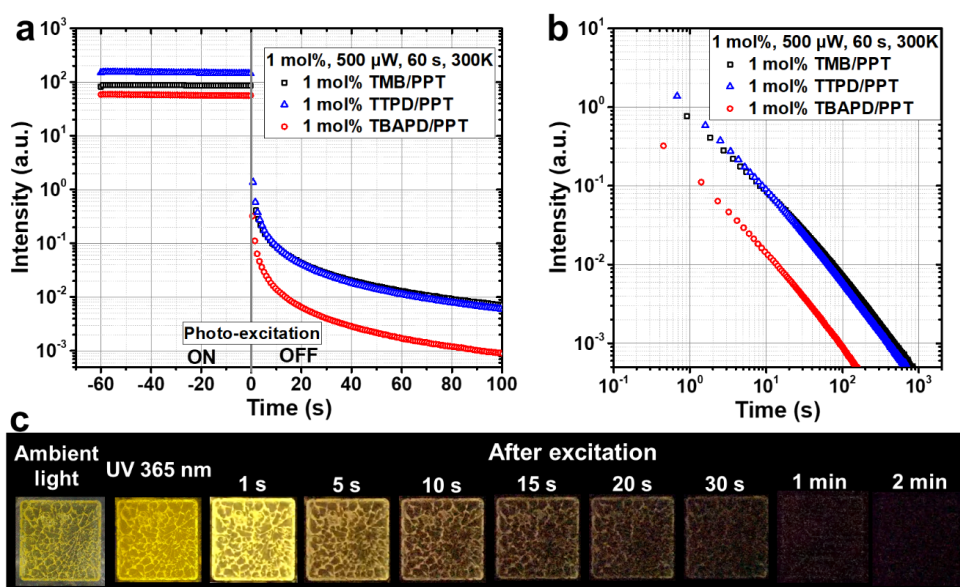
Figure 3. a, b. Semi-logarithmic plots (**a**) and logarithmic plots (**b**) of the emission decay profiles of TMB/PPT, TTPD/PPT, and TBAPD/PPT at 300 K. Samples were excited for 60 s (from −60 to 0 s) by a 340-nm LED source. "PL" means the steady-state photoluminescence, "LPL" means the long-persistent luminescence. **c**. Photographs of a 1 mol% TBAPD/PPT thick film at room temperature under the ambient light, during excitation by a 365-nm UV lamp, and at various times after turning off the excitation.

TTPD/PPT films are almost identical, although the TTPD/PPT film exhibits a higher Φ_{PL}. Because the final emission comes from the exciplex, the Φ_{PL} is important for LPL emitters. However, emission in the OLPL system occurs through charge separation process from the CT state to the CS state, charge retention in the CS state, and charge recombination process from the CS state to the CT state. Thus, differences such as charge separation probability from the CT state to the CS state between the TMB/PPT and TTPD/PPT films may lead to the difference between the LPL duration and Φ_{PL}.

In conclusion, we demonstrated orange LPL emission from the donor/acceptor binary system, TBAPD/PPT, by tuning the HOMO level of the donor. In contrast, TTPD possesses a similar HOMO level with TMB, so the TTPD/PPT and TMB/PPT blend films both exhibit green LPL emission. This approach will enable control of the LPL emission color of the donor/acceptor binary system.

Supporting Information is available on http://dx.doi.org/10.1246/cl.******.

References and Notes

1 J. Xu, S. Tanabe, *J. Lumin.* **2019**, *205*, 581.
2 *Long Afterglow Phosphorescent Materials*, ed. by S. Wu, Z. Pan, R. Chen, X. Liu, Springer, Cham, **2017**.
3 Y. Li, M. Gecevicius and J. Qiu, *Chem. Soc. Rev.*, **2016**, 45, 2090.
4 S. Xu, R. Chen, C. Zheng, W. Huang, *Adv. Mater.* **2016**, *28*, 9920.
5 T. Matsuzawa, Y. Aoki, N. Takeuchi, Y. Murayama, *J. Electrochem. Soc.* **1996**, *143*, 2670.
6 M. P. Anesh, S. K. H. Gulrez, A. Anis, H. Shaikh, M. E. Ali Mohsin, S. M. Al-Zahrani, *Adv. Polym. Tech.* **2014**, *33*, 21436.
7 Z. Lin, R. Kabe, N. Nishimura, K. Jinnai, C. Adachi, *Adv. Mater.* **2018**, *30*, 1803713.
8 R. Kabe, C. Adachi, *Nature* **2017**, *550*, 384.
9 A. Gilbert, J. E. Baggott and J. Baggott, Blackwell Scientific Publications, London, **1991**.
10 S. A. Jenekhe and J. A. Osaheni, *Science*, 1994, **265**, 765.
11 D. Kolosov, V. Adamovich, P. Djurovich, M. E. Thompson and C. Adachi, *J. Am. Chem. Soc.*, **2002**, 124, 9945.
12 X. K. Liu, Z. Chen, C. J. Zheng, C. L. Liu, C. S. Lee, F. Li, X. M. Ou and X. H. Zhang, *Adv. Mater.*, **2015**, 27, 2378.
13 J. Pommerehne, H. Vestweber, W. Guss, R. F. Mahrt, H. Bässler, M. Porsch and J. Daub, *Adv. Mater.*, **1995**, 7, 551.
14 Y. Liu, M. S. Liu and A. K.-Y. Jen, *Acta Polym.*, **1999**, 50, 105.
15 P. Debye, J. O. Edwards, *J. Chem. Phys.* **1952**, *20*, 236.
16 G. C. Abell, A. Mozumder, *J. Chem. Phys.* **1972**, *56*, 4079.
17 M. Tachiya and A. Mozumder, *Chem. Phys. Lett.*, **1975**, 34, 77.
18 Y. Hama, Y. Kimura, M. Tsumura and N. Omi, *Chem. Phys.*, **1980**, 53, 115.
19 H. Ohkita, W. Sakai, A. Tsuchida and M. Yamamoto, *Macromolecules*, **1997**, 30, 5376.
20 S. Hirata, K. Totani, J. Zhang, T. Yamashita, H. Kaji, S. R. Marder, T. Watanabe, C. Adachi, *Adv. Funct. Mater.* **2013**, *23*, 3386.
21 S. Hirata, K. Totani, T. Yamashita, C.Adachi, M. Vacha, *Nat. Mater.* **2014**, *13*, 938.
22 Z. An, C. Zheng, Y. Tao, R. Chen, H. Shi, T. Chen, Z. Wang, H. Li, R. Deng, X. Liu, W. Huang, *Nat. Mater.* **2015**, *14*, 685.
23 W. Zhao, Z. He, J.W. Y. Lam, Q. Peng, H. Ma, Z. Shuai, G. Bai, J. Hao, B. Z. Tang, *Chem* **2016**, *1*, 592.
24 H. Mieno, R. Kabe, N. Notsuka, M. D. Allendorf, C.Adachi, *Adv. Opt. Mater.* **2016**, *4*, 1015.
25 N. Notsuka, R. Kabe, K. Goushi, C. Adachi, *Adv. Funct. Mater.* **2017**, *27*, 1703902.
26 Y. Su, S. Z. F. Phua, Y. Li, X. Zhou, D. Jana, G. Liu, W. Q. Lim, W. K. Ong, C. Yang, Y. Zhao, *Sci. Adv.* **2018**, *4*, eaas9732.
27 D. Li, F. Lu, J. Wang, W. Hu, X.-M. Cao, X. Ma and H. Tian, *J. Am. Chem. Soc.*, **2018**, 140, 1916.
28 L. Gu, H. Shi, L. Bian, M. Gu, K. Ling, X. Wang, H. Ma, S. Cai, W. Ning, L. Fu, H. Wang, S. Wang, Y. Gao, W. Yao, F. Huo, Y. Tao, Z. An, X. Liu, W. Huang, *Nat. Photonics* **2019**, *13*, 406.
29 K. Jinnai, N. Nishimura, R. Kabe, C. Adachi, *Chem. Lett.* **2019**, *48*, 270.
30 K. Jinnai, R. Kabe, C. Adachi, *Adv. Mater.* **2018**, *30*, 1800365.
31 C. Fan, C. Duan, Y. Wei, D. Ding, H. Xu, W. Huang, *Chem. Mater.* **2015**, *27*, 5131.